Magneto-optical Kerr effect from layered systems when using elliptically polarized incident light

A. Vernes and P. Weinberger
Center for Computational Materials Science, Technical University Vienna, Gumpendorferstrasse 1a, A-1060 Vienna, Austria
(Received 29 January 2004; revised manuscript received 25 May 2004; published 15 October 2004)

Exploiting the dependence of Kerr spectra on the polarization state of incident light, it is shown that Kerr angles can be optimized by using elliptically polarized incident light. The proposed scheme is applied to fcc Ni(100) and fcc $Co/Pt_3/Co/Pt(100)$. By making use of the complex optical conductivity tensor (calculated by means of the spin-polarized relativistic screened Korringa-Kohn-Rostoker method) and an appropriate 2×2 matrix formalism (to include all reflections and interferences) it is found, that the Kerr angle can be increased substantially even for very small deviations from perfect normal incidence or polar geometry. This increase pertains over the entire visible range of photon energies when using almost circularly polarized incident light. In the case of Ni(100) it is shown that depending on the photon energy even in using arbitrary linearly polarized incident light of azimuth different than ±45°, the Kerr angles can be improved by 5–60 %.

DOI: 10.1103/PhysRevB.70.134411 PACS number(s): 78.20.Bh, 78.20.Ci, 78.20.Ls, 78.67.Pt

I. INTRODUCTION

In 1876 Kerr discovered that reflected from iron the polarization plane of linearly polarized light is rotated. Since in his first experiments the pole of an Fe magnet was used, this magneto-optical effect has been called the polar Kerr effect. Two years later Kerr demonstrated that the same effect shows up even when iron is magnetized in plane. This particular setup is known today as the longitudinal geometry.[1] Nowadays, the magneto-optical Kerr effect (MOKE) is a widely used powerful experimental tool, e.g., for magnetic domain imaging, mapping of hysteresis loops, etc., and technologically applied in magneto-optical high-density recording.[2]

MOKE is usually identified with a change in the polarization state of incident linearly polarized light when reflected from a magnetic system,[3] namely, with a rotation of the main polarization plane (characterized by the Kerr rotation angle θ_K) and the ellipticity of the reflected light (i.e., Kerr ellipticity e_K or equivalently to this attached ellipticity angle ϵ_K).[4,5] In viewing the linearly polarized incident light as a superposition of right- and left-handed circularly polarized waves of equal amplitudes, from a purely optical point of view, the magneto-optical Kerr effect is caused by different reflections of these two circularly polarized components of the incident light.[3,5]

Based on the relative orientation of the magnetization with respect to the surface of the system and the plane of incidence, one distinguishes between three basic Kerr geometries, which are most frequently used in experiments. In the polar Kerr effect, the magnetization of the system is in the plane of incidence and perpendicular to the reflective surface. The longitudinal (meridional) Kerr effect occurs, when the magnetization is parallel to both, the plane of incidence and the reflective surface. If the magnetization is in plane and perpendicular to the plane of incidence, the Kerr effect is said to be transverse (equatorial) and, unlike in other geometries,[4] magnetization-dependent intensity differences are measured.[5] Because only the polar Kerr effect and a specific transverse configuration goes linearly with the magnitude of magnetization,[3] presently, all optical data storage technologies use these geometries.[2] The longitudinal Kerr effect, on the other hand, is mainly applied for investigating domain structures.[4]

In principle, the magneto-optical Kerr effect has to show up also for elliptically or at least arbitrary linearly polarized incidence light. Exactly this, namely, to point out the consequences of using MOKE with elliptically polarized incidence light, is the scope of the present contribution.

The paper is organized as follows. In Sec. II an appropriate 2×2 matrix technique is introduced, which facilitates to recursively calculate the surface reflectivity matrix in the case of an arbitrary layered system. In Sec. III this surface reflectivity matrix is then used to obtain the polarization state of the reflected light for an arbitrary geometry and oblique incidence. In Sec. IV it is shown that in general the polarization state of the reflected light also depends on the polarization state of the incident light and therefore (with the exception of the ideal case of polar geometry and normal incidence) both the Kerr rotation and the Kerr ellipticity angle can easily be manipulated by using elliptically polarized incident light. Section V serves to illustrate the gain in optimizing the Kerr angles using elliptically polarized incident light. Finally, in Sec. VI the obtained results are summarized.

II. SURFACE REFLECTIVITY MATRIX

Consider a right-handed Cartesian coordinate system $S\{x,y,z\}$ with the origin fixed in the interface between vacuum and a given layered system such that the z axis is perpendicular to the surface layer and $+z$ points into the vacuum. In the following, layers are numbered starting with the first bulklike layer of a semi-infinite substrate ($p=1$), i.e., if N layers are considered, the index of the surface layer is $p=N$. It is convenient to label the substrate and the vacuum by 0 and $N+1$, respectively. Furthermore, it is assumed that the lower and upper boundaries of the layer p are planes situated at z_p and z_{p+1} ($z_p<z_{p+1}$), see also Fig. 1.

From the optical point of view each layer p can be supposed to be a homogeneous, linear and anisotropic conduct-

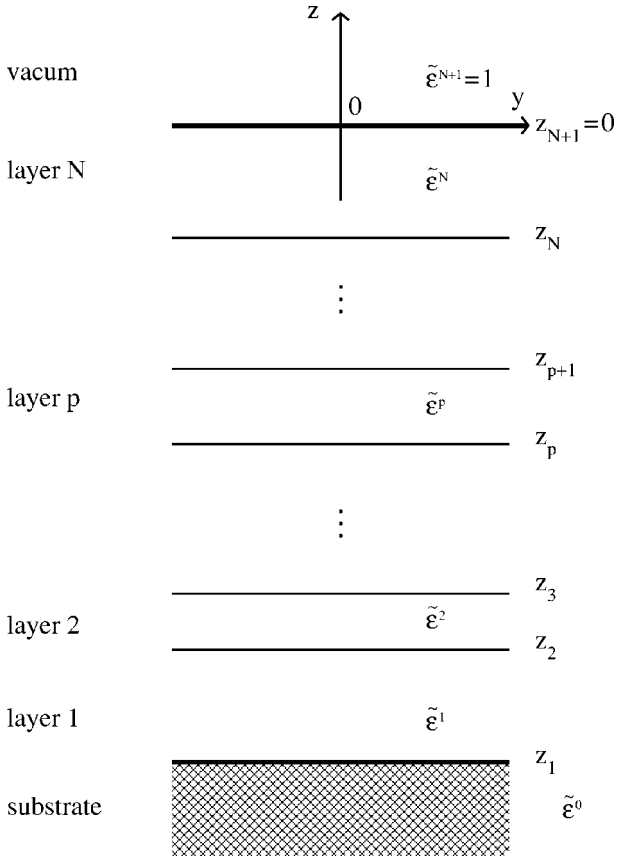

FIG. 1. The macroscopic model of a layered system used within the 2×2 matrix technique. The x axis is perpendicular to the plane of the figure.

ing medium characterized by the complex permittivity $\tilde{\varepsilon}^p(\omega)$. The plane waves associated with the complex electric and magnetic fields propagating through a layer p are given by

$$\vec{A}_p(\vec{r},t) = \vec{\mathcal{A}}_p \exp[i(\vec{q}_p\vec{r} - \tilde{\omega}t)] \ (\vec{\mathcal{A}}_p \in \mathbb{C}), \tag{1}$$

where $\vec{q}_p$ is the complex propagation vector and $\tilde{\omega}=\omega - i\delta$ is the complex frequency, with δ being a positive infinitesimal imposing the electromagnetic field to be turned on in the infinite past.[6] In terms of the spherical colatitude θ $(0\leqslant\theta<\pi/2)$ and longitude φ $(0\leqslant\varphi\leqslant 2\pi)$ of the light incident coming in from the vacuum side, $\vec{q}_p=q_0\vec{n}_p = q_0(\tilde{n}_{px}\vec{e}_x+\tilde{n}_{py}\vec{e}_y+\tilde{n}_{pz}\vec{e}_z)$, with q_0 being the propagation constant in vacuum, $\vec{e}_x$, $\vec{e}_y$, $\vec{e}_z$ the unit vectors in $S\{x,y,z\}$, and $\vec{n}_p$ being the complex refraction vector in layer p

$$\tilde{n}_{px} = -\sin\theta\cos\varphi = \tilde{n}_x,$$

$$\tilde{n}_{py} = -\sin\theta\sin\varphi = \tilde{n}_y,$$

$$\tilde{n}_{pz} = \tilde{N}_p(\omega)\cos\theta. \tag{2}$$

Within the Gaussian system of units and suppressing the frequency dependence of all quantities, the propagation of the electric and magnetic plane waves in a layer p is completely described by the Helmholtz equation[4]

$$\sum_{\nu=x,y,z} (\tilde{n}_p^2\delta_{\mu\nu} - \tilde{n}_{p\mu}\tilde{n}_{p\nu} - \tilde{\varepsilon}^p_{\mu\nu})\mathcal{E}_{p\nu} = 0, \ (\mu = x,y,z) \tag{3}$$

and the curl Maxwell equation[7]

$$\vec{\mathcal{H}}_p = \vec{n}_p \times \vec{E}_p. \tag{4}$$

Indeed, knowing the permittivity $\tilde{\varepsilon}^p(\omega)$, the normal modes (i.e., nontrivial solutions of the Helmholtz equation) are immediately obtained by solving the Fresnel (characteristic) equation[8]

$$|\tilde{n}_p^2\delta_{\mu\nu} - \tilde{n}_{p\mu}\tilde{n}_{p\nu} - \tilde{\varepsilon}^p_{\mu\nu}| = 0 \ (\mu,\nu = x,y,z), \tag{5}$$

which is of fourth order in $\tilde{n}_{pz}$ and directly results from the vanishing of the determinant of the system of linear equations in Eq. (3). For each normal mode $\tilde{n}^{(k)}_{pz}$ $(k=1,\ldots,4)$, the Helmholtz equation (3) then directly provides all Cartesian components of the electric field $\vec{\mathcal{E}}^{(k)}_p$, which in turn substituted into Eq. (4), finally yield the magnetic field $\vec{\mathcal{H}}^{(k)}_p$.

The imaginary part of $\tilde{n}^{(k)}_{pz}$, on the other hand, uniquely fixes the propagation direction of beam k in the $-z$ direction, when $\mathrm{Im}\,\tilde{n}^{(k)}_{pz}<0$, or in $+z$ direction, if $\mathrm{Im}\,\tilde{n}_{pz}>0$, see Eq. (1). In the following, $\tilde{n}^{(1)}_{pz}$ and $\tilde{n}^{(2)}_{pz}$ denote those solutions of Eq. (5), which correspond to beams propagating in direction $-z$ ("downward"), whereas $\tilde{n}^{(3)}_{pz}$ and $\tilde{n}^{(4)}_{pz}$ stand for normal modes propagating in the opposite "upward" direction.

In practice, the determination of $\vec{\mathcal{E}}^{(k)}_p$ is slightly complicated by the fact, that not all equations in Eq. (3) are linearly independent and therefore the Helmholtz equation for a given solution $\tilde{n}^{(k)}_{pz}$ of Eq. (5) has to be solved by keeping at least one Cartesian component of the electric field arbitrary. Among all possible parametrization of the electric fields in a given layer p, a physically very transparent scheme results by following Mansuripur's strategy[2,9]

$$\mathcal{E}^{(k)}_{px} = \text{arbitrary},$$

$$\mathcal{E}^{(k)}_{py} = \tilde{\alpha}^{(k)}_p\mathcal{E}^{(k)}_{px},$$

$$\mathcal{E}^{(k)}_{pz} = \tilde{\beta}^{(k)}_p\mathcal{E}^{(k)}_{px}, \ \text{for } k=1,3$$

and

$$\mathcal{E}^{(k)}_{px} = \tilde{\alpha}^{(k)}_p\mathcal{E}^{(k)}_{py},$$

$$\mathcal{E}^{(k)}_{py} = \text{arbitrary},$$

$$\mathcal{E}^{(k)}_{pz} = \tilde{\beta}^{(k)}_p\mathcal{E}^{(k)}_{py}, \quad \text{for } k=2,4. \tag{6}$$

The layer-resolved reflectivity matrix $\mathcal{R}_p$ relates then all arbitrary electric field components at the lower boundary z_p to each other as

$$\begin{pmatrix}\mathcal{E}^{(3)}_{px}\\ \mathcal{E}^{(4)}_{py}\end{pmatrix} = \mathcal{R}_p\begin{pmatrix}\mathcal{E}^{(1)}_{px}\\ \mathcal{E}^{(2)}_{py}\end{pmatrix} = \begin{pmatrix}\tilde{r}^p_{11} & \tilde{r}^p_{12}\\ \tilde{r}^p_{21} & \tilde{r}^p_{22}\end{pmatrix}\begin{pmatrix}\mathcal{E}^{(1)}_{px}\\ \mathcal{E}^{(2)}_{py}\end{pmatrix}, \ p=0,\ldots,N+1. \tag{7}$$

By exploiting in each layer $p=0,\ldots,N+1$ the continuity of the tangential components of the total electric and magnetic

field at the lower boundary z_p, the reflectivity matrices

$$\mathcal{R}_p = (\mathcal{D}_{p-1}\mathcal{A}_p^{34} - \mathcal{B}_p^{34})^{-1}(\mathcal{B}_p^{12} - \mathcal{D}_{p-1}\mathcal{A}_p^{12}) \tag{8}$$

can be determined recursively by starting from the vanishing reflectivity matrix $\mathcal{R}_0=0$ of the substrate (viewed as a semi-infinite bulk without boundaries) and by means of the following 2×2 matrices

$$\mathcal{A}_p^{k,k+1} = \begin{pmatrix} 1 & \tilde{\alpha}_p^{(k+1)} \\ \tilde{\alpha}_p^{(k)} & 1 \end{pmatrix},$$

$$\mathcal{B}_p^{k,k+1} = \begin{pmatrix} \tilde{n}_y\tilde{\beta}_p^{(k)} - \tilde{n}_{pz}^{(k)}\tilde{\alpha}_p^{(k)} & \tilde{n}_y\tilde{\beta}_p^{(k+1)} - \tilde{n}_{pz}^{(k+1)} \\ \tilde{n}_{pz}^{(k)} - \tilde{n}_x\tilde{\beta}_p^{(k)} & \tilde{n}_{pz}^{(k+1)}\tilde{\alpha}_p^{(k+1)} - \tilde{n}_x\tilde{\beta}_p^{(k+1)} \end{pmatrix}, \tag{9}$$

where $\tilde{\alpha}_p^{(k)}$ and $\tilde{\beta}_p^{(k)}$ refer to Eq. (6) and $\vec{n}_p$ to Eq. (2). Furthermore, also the propagation matrices

$$\mathcal{C}_p^{k,k+1} = \begin{pmatrix} \exp[+iq_0\tilde{n}_{pz}^{(k)}d_p] & 0 \\ 0 & \exp[+iq_0\tilde{n}_{pz}^{(k+1)}d_p] \end{pmatrix},$$

$$(k = 1,3 \text{ and } p = 0, \ldots, N), \tag{10}$$

with $d_p=z_{p+1}-z_p>0$ being the thickness of layer p, are needed to construct the auxiliary matrices

$$\mathcal{D}_p = (\mathcal{B}_p^{12}\mathcal{C}_p^{12} + \mathcal{B}_p^{34}\mathcal{C}_p^{34}\mathcal{R}_p)(\mathcal{A}_p^{12}\mathcal{C}_p^{12} + \mathcal{A}_p^{34}\mathcal{C}_p^{34}\mathcal{R}_p)^{-1},$$

$$p = 0, \ldots, N \tag{11}$$

to be used. Because in vacuum there are only two normal modes, namely an incident beam ($\tilde{n}_{N+1,z}^{(1)}=\tilde{n}_{N+1,z}^{(2)}=\tilde{n}_{N+1,z}^{(\mathrm{i})}$) and reflected beam ($\tilde{n}_{N+1,z}^{(3)}=\tilde{n}_{N+1,z}^{(4)}=\tilde{n}_{N+1,z}^{(\mathrm{r})}$), the surface reflectivity matrix is given by

$$\mathcal{R}_{\mathrm{surf}} = R_{N+1} = (\mathcal{D}_N - \mathcal{B}_{N+1}^{34})^{-1}(\mathcal{B}_{N+1}^{12} - \mathcal{D}_N) = \begin{pmatrix} \tilde{r}_{xx} & \tilde{r}_{xy} \\ \tilde{r}_{yx} & \tilde{r}_{yy} \end{pmatrix}, \tag{12}$$

where in terms of Eq. (9),

$$\mathcal{B}_{N+1}^{12} = -\mathcal{B}_{N+1}^{34} = \frac{1}{\sqrt{1-(\tilde{n}_x^2+\tilde{n}_y^2)}}\begin{pmatrix} \tilde{n}_x\tilde{n}_y & 1-\tilde{n}_x^2 \\ -1+\tilde{n}_y^2 & -\tilde{n}_x\tilde{n}_y \end{pmatrix}. \tag{13}$$

$\mathcal{R}_{\mathrm{surf}}$ then relates the tangential components of the reflected light with respect to the reference frame $S\{x,y,z\}$ to the corresponding components of the incident light

$$\begin{pmatrix} \mathcal{E}_{N+1,x}^{(\mathrm{r})} \\ \mathcal{E}_{N+1,y}^{(\mathrm{r})} \end{pmatrix} = \mathcal{R}_{\mathrm{surf}} = \begin{pmatrix} \mathcal{E}_{N+1,x}^{(\mathrm{i})} \\ \mathcal{E}_{N+1,y}^{(\mathrm{i})} \end{pmatrix} = \begin{pmatrix} \tilde{r}_{xx}\mathcal{E}_{N+1,x}^{(\mathrm{i})} + \tilde{r}_{xy}\mathcal{E}_{N+1,y}^{(\mathrm{i})} \\ \tilde{r}_{yx}\mathcal{E}_{N+1,x}^{(\mathrm{i})} + \tilde{r}_{yy}\mathcal{E}_{N+1,y}^{(\mathrm{i})} \end{pmatrix}. \tag{14}$$

Hence in contrast to the layer-resolved reflectivity matrices $\mathcal{R}_p$ for $\forall p=0,\ldots,N$ as introduced in Eq. (7), here the complex reflectivity coefficient $\tilde{r}_{\mu\nu}$ is the fraction of the νth component of the incident electric field contained in the μth component of the reflected electric field ($\mu,\nu=x,y$).

For a homogeneous layered system consisting of identical layers from Eqs. (8) and (11) immediately follows that all layer-resolved reflectivity matrices are vanishing, i.e., $\mathcal{R}_p=0$ for $\forall p=0,\ldots,N$. This in turn implies that for a semi-infinite bulk system, the surface reflectivity matrix with respect to the reference frame $S\{x,y,z\}$ is simply given by[10]

$$\mathcal{R}_{\mathrm{surf}}^{(b)} = [\mathcal{B}_{N+1}^{12} + \mathcal{B}_b^{12}(\mathcal{A}_b^{12})^{-1}]^{-1}[\mathcal{B}_{N+1}^{12} - \mathcal{B}_b^{12}(\mathcal{A}_b^{12})^{-1}]. \tag{15}$$

III. POLARIZATION STATE OF TRANSVERSE PLANE WAVES

The polarization state of a wave describes the time dependence of the electric field vector at a given point in space. In order to determine the polarization state of transverse plane waves, one primarily has to know the electric field components in a plane perpendicular to the propagation direction. Consider a local right-handed Cartesian coordinate system $L\{p,s,d\}$, attached to the investigated wave, with the d axis pointing along the propagation direction, the p axis being in the plane of incidence (perpendicular to d axis) and the s axis perpendicular to plane of incidence (perpendicular to both d and p axes).

A transformation of $S\{x,y,z\}$ to $L\{p,s,d\}$ consists of two successive rotations: a rotation around the z axis by an angle φ followed by a rotation by the angle between the propagation direction of the wave and the z axis around the new y' axis. Note that only in vacuum for this angle $\theta=\theta_{N+1}^{(\mathrm{i})}=-\theta_{N+1}^{(\mathrm{r})}$ implies and therefore

$$\begin{pmatrix} \mathcal{E}_{N+1,x}^{(k)} \\ \mathcal{E}_{N+1,y}^{(k)} \end{pmatrix} = \mathcal{P}_{N+1}^{(k)} = \begin{pmatrix} \mathcal{E}_{N+1,p}^{(k)} \\ \mathcal{E}_{N+1,s}^{(k)} \end{pmatrix} + \begin{pmatrix} \cos\theta\cos\varphi & -\sin\varphi \\ \cos\theta\sin\varphi & \cos\varphi \end{pmatrix} \times \begin{pmatrix} \mathcal{E}_{N+1,p}^{(k)} \\ \mathcal{E}_{N+1,s}^{(k)} \end{pmatrix} (k = i,r),$$

see Eq. (2). By introducing the 2×2 rotation matrix

$$\mathcal{P}_{N+1} \equiv \mathcal{P}_{N+1}^{(\mathrm{i})} = \mathcal{P}_{N+1}^{(\mathrm{r})},$$

the surface reflectivity matrix is then given by

$$\mathsf{R}_{\mathrm{surf}} = \mathcal{P}_{N+1}^{-1}\mathcal{R}_{\mathrm{surf}}\mathcal{P}_{N+1} = \begin{pmatrix} \tilde{r}_{pp} & \tilde{r}_{ps} \\ \tilde{r}_{sp} & \tilde{r}_{ss} \end{pmatrix}. \tag{16}$$

Consequently the complex reflectivity coefficients, see also Eq. (12), are given by

$$\tilde{r}_{pp} = \tilde{r}_{xx}\cos^2\varphi + \tilde{r}_{yy}\sin^2\varphi + (\tilde{r}_{xy}+\tilde{r}_{yx})\sin\varphi\cos\varphi,$$

$$\tilde{r}_{ps} = [\tilde{r}_{xy}\cos^2\varphi - \tilde{r}_{yx}\sin^2\varphi + (\tilde{r}_{yy}-\tilde{r}_{xx})\sin\varphi\cos\varphi]\frac{1}{\cos\theta},$$

$$\tilde{r}_{sp} = [\tilde{r}_{yx}\cos^2\varphi - \tilde{r}_{xy}\sin^2\varphi + (\tilde{r}_{yy}-\tilde{r}_{xx})\sin\varphi\cos\varphi]\cos\theta,$$

$$\tilde{r}_{ss} = \tilde{r}_{yy}\cos^2\varphi + \tilde{r}_{xx}\sin^2\varphi - (\tilde{r}_{xy}+\tilde{r}_{yx})\sin\varphi\cos\varphi \tag{17}$$

and now directly relate the p and s components of the reflected wave to that of the incident one

$$\begin{pmatrix} \mathcal{E}^{(\mathrm{r})}_{N+1,p} \\ \mathcal{E}^{(\mathrm{r})}_{N+1,s} \end{pmatrix} = \mathsf{R}_{\mathrm{surf}} \begin{pmatrix} \mathcal{E}^{(\mathrm{i})}_{N+1,p} \\ \mathcal{E}^{(\mathrm{i})}_{N+1,s} \end{pmatrix} = \begin{pmatrix} \tilde{r}_{pp}\mathcal{E}^{(\mathrm{i})}_{N+1,p} + \tilde{r}_{ps}\mathcal{E}^{(\mathrm{i})}_{N+1,s} \\ \tilde{r}_{sp}\mathcal{E}^{(\mathrm{i})}_{N+1,p} + \tilde{r}_{ss}\mathcal{E}^{(\mathrm{i})}_{N+1,s} \end{pmatrix}. \tag{18}$$

In contrast to Eq. (14), for a given $\tilde{r}_{\mu\nu}$ here $\nu \in L^{(\mathrm{i})}\{p,s,d\}$ (coordinate system of the incident electric field) and $\mu \in L^{(\mathrm{r})}\{p,s,d\}$ (coordinate system of the reflected electric field). Although in principle, $L^{(\mathrm{r})}\{p,s,d\}$ is not identical with $L^{(\mathrm{i})}\{p,s,d\}$, for a vanishing d component of the electric field, the difference between $L^{(\mathrm{r})}\{p,s,d\}$ and $L^{(\mathrm{i})}\{p,s,d\}$ is of minor importance. Therefore, in the following $\mathsf{R}_{\mathrm{surf}}$ is simply termed the surface reflectivity matrix with respect to the local Cartesian coordinate system $L\{p,s,d\}$.

To calculate the Kerr rotation and ellipticity angle, one has to determine the polarization state of the reflected light in terms of the Cartesian components $\mathcal{E}^{(r)}_{N+1,p}$ and $\mathcal{E}^{(r)}_{N+1,s}$ of the reflected electric field. These are immediately obtained via Eq. (18), if in addition to the surface reflectivity matrix $\mathcal{R}_{\mathrm{surf}}$ with respect to $S\{x,y,z\}$, see Eq. (12) and the geometry of the incidence, the polarization state of the incident light is also known. However, because the polarization state of any monochromatic, transverse wave is completely specified within $L\{p,s,d\}$ by the amplitude $|\mathcal{E}|$, the absolute phase ϕ, the azimuth ϑ and ellipticity angle ε, namely,[11]

$$\begin{pmatrix} \mathcal{E}_p \\ \mathcal{E}_s \end{pmatrix} = \mathcal{E} \begin{pmatrix} \cos\vartheta\cos\varepsilon - i\sin\vartheta\sin\varepsilon \\ \sin\vartheta\cos\varepsilon + i\cos\vartheta\sin\varepsilon \end{pmatrix}, \tag{19}$$

where

$$\mathcal{E} = |\mathcal{E}|\exp(i\phi)$$

and

$$-\frac{\pi}{2} \leqslant \vartheta \leqslant \frac{\pi}{2} \text{ and } -\frac{\pi}{4} \leqslant \varepsilon \leqslant \frac{\pi}{4}, \tag{20}$$

it follows that all these quantities have to be specified for the incident light, in order to get the polarization state of the light reflected from a layered system. For example, an arbitrary linearly polarized incident wave is present, if its ellipticity is zero and hence the Cartesian Jones vector in Eq. (18) is of the form

$$\begin{pmatrix} \mathcal{E}^{(i)}_{N+1,p} \\ \mathcal{E}^{(i)}_{N+1,s} \end{pmatrix} = \mathcal{E}_i \begin{pmatrix} \cos\vartheta_i \\ \sin\vartheta_i \end{pmatrix}, \tag{21}$$

while a right-handed (left-handed) circular incident wave corresponds to $\varepsilon_i = +\pi/4(-\pi/4)$ and

$$\begin{pmatrix} \mathcal{E}^{(i)}_{N+1,p} \\ \mathcal{E}^{(i)}_{N+1,s} \end{pmatrix} = \pm\frac{\mathcal{E}_i}{\sqrt{2}} \begin{pmatrix} \exp(-i\vartheta_i) \\ \exp(+i\vartheta_i) \end{pmatrix}. \tag{22}$$

As long as in Eq. (22) the azimuth of the incident wave ϑ_i is indeterminable, the quantity in Eq. (21) defines the handedness of the arbitrary linearly polarized incident wave. In particular for a p wave $\vartheta_i = 0$; for a right-handed (left-handed) s wave, $\vartheta_i = +\pi/2(-\pi/2)$.

IV. KERR ROTATION AND ELLIPTICITY ANGLE

Because the magneto-optical Kerr effect is fully described by the Kerr rotation angle and ellipticity angle, the amplitude and the absolute phase of the incident and the reflected light are of secondary interest. From Eq. (19) one immediately can see that by dividing the components of the Jones vector by each other, a simpler representation of the polarization state is obtained, which directly provides the azimuth and the ellipticity angle of any monochromatic transverse wave and hence the Kerr rotation and ellipticity angles.[11] Defining therefore the polarization variable of the incident wave within the Cartesian complex plane as

$$\tilde{\chi}^{(i)}_{[p,s]} = \frac{\mathcal{E}^{(i)}_{N+1,s}}{\mathcal{E}^{(i)}_{N+1,p}} = \frac{\tan\vartheta_i + i\tan\varepsilon_i}{1 - i\tan\vartheta_i\tan\varepsilon_i},$$

from Eq. (18) follows that the polarization variable $\tilde{\chi}^{(r)}_{[p,s]}$ of the reflected wave can be written as

$$\begin{aligned} \tilde{\chi}^{(r)}_{[p,s]} &= \frac{\mathcal{E}^{(r)}_{N+1,s}}{\mathcal{E}^{(r)}_{N+1,p}} = \frac{\tilde{r}_{sp}\mathcal{E}^{(i)}_{N+1,p} + \tilde{r}_{ss}\mathcal{E}^{(i)}_{N+1,s}}{\tilde{r}_{pp}\mathcal{E}^{(i)}_{N+1,p} + \tilde{r}_{ps}\mathcal{E}^{(i)}_{N+1,s}} = \frac{\tilde{r}_{sp} + \tilde{r}_{ss}\tilde{\chi}^{(i)}_{[p,s]}}{\tilde{r}_{pp} + \tilde{r}_{ps}\tilde{\chi}^{(i)}_{[p,s]}} \\ &= \frac{\tilde{r}_{sp}(1 - i\tan\vartheta_i\tan\varepsilon_i) + \tilde{r}_{ss}(\tan\vartheta_i + i\tan\varepsilon_i)}{\tilde{r}_{pp}(1 - i\tan\vartheta_i\tan\varepsilon_i) + \tilde{r}_{ps}(\tan\vartheta_i + i\tan\varepsilon_i)}. \end{aligned} \tag{23}$$

The azimuth ϑ_r and ellipticity angle ε_r of the reflected light are then directly obtained from the following expressions:

$$\tan 2\vartheta_r = \frac{2\,\mathrm{Re}(\tilde{\chi}^{(r)}_{[p,s]})}{1 - |\tilde{\chi}^{(r)}_{[p,s]}|^2} \text{ and } \sin 2\varepsilon_r = \frac{2\,\mathrm{Im}(\tilde{\chi}^{(r)}_{[p,s]})}{1 + |\tilde{\chi}^{(r)}_{[p,s]}|^2}. \tag{24}$$

In particular, if the incident light is a p wave, i.e., $\vartheta_i = \varepsilon_i = 0$, Eq. (23) reduces to $\tilde{\chi}^{(r)}_{[p,s]} = \tilde{r}_{sp}/\tilde{r}_{pp}$, and the Kerr rotation angle $\theta_{K,p} = \vartheta_r$, whereas the Kerr ellipticity $\epsilon_{K,p} = \varepsilon_r$. Because normally both Kerr angles are small, $\tan 2\theta_K \simeq 2\theta_K$ and $\sin 2\epsilon_K \simeq 2\epsilon_K$, and in addition $|\tilde{\chi}^{(r)}_{[p,s]}|^2 \ll 1$, Eq. (24) directly provides the below approximation for the complex Kerr angle

$$\Phi_{K,p} = \theta_{K,p} + i\epsilon_{K,p} \simeq \frac{\tilde{r}_{sp}}{\tilde{r}_{pp}} \text{ (incident } p \text{ wave)}, \tag{25}$$

with $\theta_{K,p}$ referring to the positive p axis.

Similarly, if the incident s wave, i.e., $\vartheta_i = \pm\pi/2$ and $\varepsilon_i = 0$, yields small Kerr rotation and ellipticity angles and $|\tilde{\chi}^{(r)}_{[p,s]}|^2 \gg 1$, from Eq. (24) immediately follows that

$$\Phi_{K,s} = -(\theta_{K,s} - i\epsilon_{K,s}) \simeq -\frac{\tilde{r}_{ps}}{\tilde{r}_{ss}} \text{ (incident } s \text{ wave)}. \tag{26}$$

By comparing for an incident s wave, the polarization variable $\tilde{\chi}^{(r)}_{[p,s]} = \tilde{r}_{ss}/\tilde{r}_{ps}$ in Eq. (23) with the expression in Eq. (26), it is evident that in Eq. (26) $\theta_{K,s}$ is measured with respect to the s axis. These rather well-known expressions for the complex Kerr angle Φ_K for a p or s incidence,[12] are nowadays widely used with different sign conventions in calculating theoretical Kerr spectra.[13–15]

Alternatively to Eq. (24), the polarization variable of the reflected wave within a complex polar coordinate system can be written as

$$\tilde{\chi}^{(r)}_{[+,-]} = \frac{i + \tilde{\chi}^{(r)}_{[p,s]}}{i - \tilde{\chi}^{(r)}_{[p,s]}} = \frac{\tilde{r}^{[p]}_{+}(1 - i\tan\vartheta_i \tan\varepsilon_i) - i\tilde{r}^{[s]}_{+}(\tan\vartheta_i + i\tan\varepsilon_i)}{\tilde{r}^{[p]}_{-}(1 - i\tan\vartheta_i \tan\varepsilon_i) + i\tilde{r}^{[s]}_{-}(\tan\vartheta_i + i\tan\varepsilon_i)}, \tag{27}$$

where

$$\begin{aligned} \tilde{r}^{[p]}_{\pm} &= \tilde{r}_{pp} \mp i\tilde{r}_{sp} = R^{[p]}_{\pm} + iI^{[p]}_{\pm} \\ \tilde{r}^{[s]}_{\pm} &= \tilde{r}_{ss} \pm i\tilde{r}_{ps} = R^{[s]}_{\pm} + iI^{[s]}_{\pm} \end{aligned} \quad (R^{[k]}_{\pm}, I^{[k]}_{\pm} \in \mathbb{R},\ k = p,s), \tag{28}$$

and the azimuth ϑ_r and the ellipticity angle ε_r are given by

$$\vartheta_r = -\frac{1}{2}\arg(\tilde{\chi}^{(r)}_{[+,-]}) \text{ and } \tan\varepsilon_r = \frac{|\tilde{\chi}^{(r)}_{[+,-]}| - 1}{|\tilde{\chi}^{(r)}_{[+,-]}| + 1}. \tag{29}$$

By using the well-known properties of complex numbers,[16] these expressions can be rewritten as

$$\vartheta_r = \frac{1}{2}(\vartheta_+ - \vartheta_-), \text{ with } \vartheta_\pm = \arctan\left(\frac{Y_\pm}{X_\pm}\right),$$

$$\tan\varepsilon_r = \frac{Z_+ - Z_-}{Z_+ + Z_-},\ Z_\pm = \sqrt{X^2_\pm + Y^2_\pm}, \tag{30}$$

where

$$\begin{aligned} X_\pm &= (R^{[p]}_\pm \pm R^{[s]}_\pm \tan\varepsilon_i) + (I^{[p]}_\pm \tan\varepsilon_i \pm I^{[s]}_\pm)\tan\vartheta_i, \\ Y_\pm &= (R^{[p]}_\pm \tan\varepsilon_i \pm R^{[s]}_\pm)\tan\vartheta_i - (I^{[p]}_\pm \pm I^{[s]}_\pm \tan\varepsilon_i). \end{aligned} \tag{31}$$

These equations show that both angles ϑ_r and ε_r also depend on the azimuth ϑ_i and the ellipticity angle ε_i of the incident light. In accordance with Eq. (20), the definition of the Kerr rotation angle θ_K then simply reduces to

$$\theta_K = \vartheta_r - \vartheta_i, \text{ where } \vartheta_k \in \left[-\frac{\pi}{2}, \frac{\pi}{2}\right] (k = i,r). \tag{32}$$

As can be seen from Eq. (27), Eqs. (30) and (35), the dependence of the Kerr angles on the incident polarization state not necessarily is linear. In general, the Kerr rotation angle as given by Eq. (32), is a function of ε_i and the incidence azimuth ϑ_i. It can be demonstrated, however, see Appendix A, that the extrema of the Kerr angle show up for an *s* or *p* wave if and only if

$$\sum_{j=\pm} \frac{R^{[p]}_j R^{[s]}_j + I^{[p]}_j I^{[s]}_j}{(R^{[s]}_j)^2 + (I^{[s]}_j)^2} = 2 \text{ or } \sum_{j=\pm} \frac{R^{[p]}_j R^{[s]}_j + I^{[p]}_j I^{[s]}_j}{(R^{[p]}_j)^2 + (I^{[p]}_j)^2} = 2, \tag{33}$$

namely for particular combinations of incidence and optical properties of the system. This in turn implies that at least in principle, the Kerr rotation angle can be enhanced by using adequate elliptically polarized incident light.

In the following, in analogy with Eq. (32), the Kerr ellipticity angle is defined as

$$\epsilon_K = \varepsilon_r - \varepsilon_i, \text{ with } \varepsilon_k \in \left[-\frac{\pi}{4}, \frac{\pi}{4}\right] (k = i,r), \tag{34}$$

namely, as the change in the ellipticity measured for reflected light with respect to that of the incident light. No doubt, that with this definition of the Kerr ellipticity angle, its physical meaning is radically changed: $\epsilon_K(\omega) = 0$, e.g., now not necessarily means that the reflected light is linearly polarized, but that both the reflected and incident light have the same ellipticity. The Kerr ellipticity angle in Eq. (34), in general depends on ϑ_i as well as on ε_i, and hence its value, at least in principle, can be increased. An exception from this occurs when using a circularly polarized incident light ($\varepsilon_i = \pm\pi/4$), because then the corresponding polarization variable of the reflected wave, see Eqs. (27) and (28), is given by

$$\tilde{\chi}^{(r)}_{[+,-]} = \frac{\tilde{r}^{[p]}_{+} \pm \tilde{r}^{[s]}_{+}}{\tilde{r}^{[p]}_{-} \mp \tilde{r}^{[s]}_{-}} = \frac{(\tilde{r}_{pp} \pm \tilde{r}_{ss}) - i(\tilde{r}_{sp} \mp i\tilde{r}_{ps})}{(\tilde{r}_{pp} \mp \tilde{r}_{ss}) + i(\tilde{r}_{sp} \pm \tilde{r}_{ps})},$$

and, independent of the handedness of the incident wave, no longer is a function of an indeterminable azimuth ϑ_i. This feature limits the validity of Eq. (32) to cases for which the ellipticity angle $\varepsilon_i \neq \pm\pi/4$!

Consider for example the particular case of polar geometry, when the magnetization in each layer $\vec{M}_p \| [001]$, and normal incidence ($\theta = 0$ and $0 \leqslant \varphi \leqslant 2\pi$). For this technological important Kerr setup, it has been shown, Ref. 17 that the surface reflectivity matrix $\mathcal{R}_{\text{surf}}$ with respect to the global coordinate system $S\{x,y,z\}$, see Eq. (12), is given by

$$\mathcal{R}_{\text{surf}} = \begin{pmatrix} \tilde{r}_{xx} & \tilde{r}_{xy} \\ -\tilde{r}_{xy} & \tilde{r}_{xx} \end{pmatrix}. \tag{35}$$

In fact, it can be easily proven (not shown in here), that $\mathcal{R}_{\text{surf}}$ is of this highly symmetric form, if and only if, the incidence is normal and the geometry is polar. In terms of Eqs. (16) and (17), the surface reflectivity matrix R_{surf} with respect to the local frame $L\{p,s,d\}$ is then identical to $\mathcal{R}_{\text{surf}}$ and, as expected, is independent of φ. For this particular case Eq. (28) yields

$$\tilde{r}^{[p]}_{\pm} = \tilde{r}^{[s]}_{\pm} = \tilde{r}_{xx} \pm i\tilde{r}_{xy} = \tilde{r}_\pm = r_\pm \exp(i\Delta_\pm), \tag{36}$$

which in turn implies that the polarization variable of the reflected wave in Eq. (27) can be be written as

$$\tilde{\chi}^{(r)}_{[+,-]} = \left[\frac{r_+}{r_-}\tan\left(\varepsilon_i + \frac{\pi}{4}\right)\right]\exp[i(\Delta_+ - \Delta_- - 2\vartheta_i)]. \tag{37}$$

For $\tilde{\chi}^{(r)}_{[+,-]}$, Eq. (29) directly leads to

$$\vartheta_r = -\frac{1}{2}(\Delta_+ - \Delta_-) + \vartheta_i \text{ and } \tan\varepsilon_r = \frac{r_+\tan\left(\varepsilon_i + \frac{\pi}{4}\right) - r_-}{r_+\tan\left(\varepsilon_i + \frac{\pi}{4}\right) + r_-}. \tag{38}$$

The Kerr angles are therefore given by

$$\theta_K = -\frac{1}{2}(\Delta_+ - \Delta_-) \text{ and } \tan \epsilon_K = \frac{r_+ - r_-}{r_+ \tan\left(\varepsilon_i + \frac{\pi}{4}\right) - r_- \tan\left(\varepsilon_i - \frac{\pi}{4}\right)}. \quad (39)$$

Alternatively, these expressions can be derived from Eqs. (30) and (31) by using $R_\pm^{[p]} = R_\pm^{[s]} = R_\pm$ and $I_\pm^{[p]} = I_\pm^{[s]} = I_\pm$. For polar geometry and normal incidence, one then gets

$$\vartheta_\pm = \pm(\vartheta_i \mp \Delta_+), \text{ where } \Delta_\pm = \arctan\left(\frac{I_\pm}{R_\pm}\right),$$

$$Z_\pm = r_\pm(1 \pm \tan \varepsilon_i)\sqrt{1 + \tan^2 \vartheta_i}, \; r_\pm = \sqrt{R_\pm^2 + I_\pm^2}.$$

Obviously, for polar geometry and normal incidence the conditions in Eq. (33) are fulfilled, implying that extrema of the Kerr rotation angle can be reached using either an incident *s* or a *p* wave. In contrast to the Kerr rotation angle for the polar geometry and normal incidence, which is not at all affected by the polarization state of the incidence light, the Kerr ellipticity depends on the ellipticity of the incidence light, such that whenever $r_+ \neq r_-$ the condition

$$\frac{\partial \epsilon_K}{\partial \varepsilon_i} = -(r_+ - r_-)\frac{r_+(1 + \tan \varepsilon_i)^2 - r_-(1 - \tan \varepsilon_i)^2}{r_+^2(1 + \tan \varepsilon_i)^2 + r_-^2(1 - \tan \varepsilon_i)^2} = 0,$$

corresponds to

$$\varepsilon_i = \arctan\left(\pm 2\frac{\sqrt{r_+ r_-}}{r_+ - r_-} - \frac{r_+ + r_-}{r_+ - r_-}\right).$$

Another interesting aspect follows directly from Eqs. (38) and (39), namely, that the polarization state of a circularly polarized incident light ($\varepsilon_i = \pm \pi/4$) after reflection is preserved, $\tan \varepsilon_r|_{\varepsilon_i = \pm \pi/4} = \pm 1$, and consequently the Kerr ellipticity as introduced in Eq. (34) vanishes, i.e., $\tan \epsilon_K|_{\varepsilon_i = \pm \pi/4} = 0$. Finally, it should be pointed out, that the expression of θ_K and that of ϵ_K for $\varepsilon_i = 0$,

$$\tan \epsilon_K = \tan \varepsilon_r = \frac{r_+ - r_-}{r_+ + r_-},$$

is well known in the literature, see for example Ref. 3. Viewed oppositely, this also means that any deviation from the polar geometry or normal incidence introduces an incident polarization dependence (ϑ_i and ε_i) for both Kerr angles θ_K and ϵ_K.

V. RESULTS AND DISCUSSIONS

From the layer-resolved optical conductivities $\tilde{\boldsymbol{\sigma}}^p(\omega)$ and for plane waves as given by Eq. (1), the layer-dependent permittivities $\tilde{\boldsymbol{\varepsilon}}^p(\omega)$ are obtained within the Gaussian system of units as [10]

$$\tilde{\boldsymbol{\varepsilon}}^p(\omega) = \boldsymbol{I} + \frac{4\pi i}{\tilde{\omega}}\tilde{\boldsymbol{\sigma}}^p(\omega),$$

where $\mathbf{I}$ is the 3×3 identity matrix

$$\tilde{\boldsymbol{\sigma}}^p(\omega) = \sum_{q=1}^{N} \tilde{\boldsymbol{\sigma}}^{pq}(\omega), \; p = 1, \ldots, N$$

and

$$\tilde{\boldsymbol{\sigma}}^{pq}(\omega) = \frac{\tilde{\boldsymbol{\Sigma}}^{pq}(\omega) - \tilde{\boldsymbol{\Sigma}}^{pq}(0)}{\hbar\omega + i\delta}, \; p,q = 1, \ldots, N,$$

with $\tilde{\boldsymbol{\Sigma}}^{pq}(\omega)$ being the current-current correlation functions.[6,18]

In the present calculations, the current-current correlation functions are numerically evaluated[19] by performing contour integrations in the complex energy plane at a finite temperature;[20] the electronic Green's function entering the kernel of these integrals is determined within the spin-polarized relativistic screened Korringa-Kohn-Rostoker (SKKR) method for layered systems.[21] The 2×2 matrix technique was applied as presented in Sec. II; the polarization state of the reflected light is directly calculated using Eqs. (27) and (29).

In the next section the dependence of Kerr rotation and ellipticity angles on the polarization state of the incident light is investigated for two Kerr setups different from an ideal polar geometry and normal incidence. In the first setup, referred to as the case of polar geometry and almost normal incidence, the geometry remains polar because of the system considered, namely fcc Ni(100), and an angle of incidence of 2° is assumed, which typically applies in standard Kerr equipments.[3] In the other setup, referred to as almost polar geometry and normal incidence, the angle of incidence vanishes, since the direction of the magnetic moments of the magneto-optically active layers in the fcc layered system $Co/Pt_3/Co/Pt_7/Pt(111)$ are chosen to be not perpendicular to the surface, but form an angle of 2° with respect to the surface normal.

A. Polar geometry and almost normal incidence

Consider fcc Ni(100) with the magnetization pointing along the *z* axis (perpendicular to the surface), i.e., polar geometry. Consider further an almost normal incidence, namely when $\tilde{n}_x$ and $\tilde{n}_y$ in Eq. (2) are not simultaneously vanishing, but the angle of incidence θ is small, e.g., 2°. This angle of incidence, $\theta = 2°$, is small enough not to yield any notable differences, whenever the incident light is linearly polarized. However it is large enough to point out the dependence of the Kerr angles on the polarization state of the incident light, see Figs. 2 and 3.

Due to nonsimultaneously vanishing *x* and *y* components of the complex refraction vector, see Eqs. (9) and (13), the surface reflectivity matrix $\mathcal{R}_{\text{surf}}$ as determined in terms of Eq. (12) with respect to the reference frame $S\{x,y,z\}$ is of lower symmetry than that defined in Eq. (35) and therefore the Kerr angles quite obviously do depend on the incident polarization state. Although in general for polar geometry and arbitrary oblique incidence, this is valid, in the case of almost normal incidence these arguments fail to explain the dependence of the polar Kerr angles on ϑ_i and ε_i. The reason of this failure is that for polar geometry and almost normal

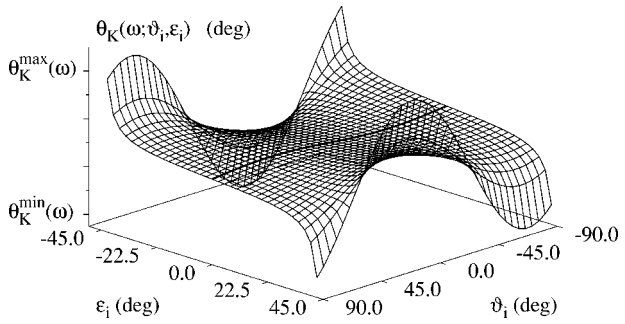

FIG. 2. Polar Kerr angle for almost normal incidence ($\theta=2°$) and arbitrary photon energies ω within the visible spectrum in the case of fcc Ni(100) as a function of the polarization state of the incident light characterized by the azimuth ϑ_i and the ellipticity angle ϵ_i. The solid bold line represents the Kerr angle calculated for arbitrary linearly polarized light ($\epsilon_i=0$). For $\omega=5$ eV, for example, $\theta_K^{\max}$ is at 0.3° and $\theta_K^{\min}$ at −0.45°.

incidence, Eq. (35) approximately is still valid, namely,

$$\tilde{r}_{yy} \simeq \tilde{r}_{xx},$$

$$\tilde{r}_{yx} \simeq -\tilde{r}_{xy} \ (\vec{M}_p \| [001] \text{ and } \theta \ll 1) \tag{40}$$

and consequently the polar Kerr spectra are independent of the longitude φ. The surface reflectivity matrix R_{surf} with respect to the local Cartesian coordinate system $L\{p,s,d\}$,

$$\mathsf{R}_{\text{surf}} \simeq \mathcal{R}_{\text{surf}} + \tilde{r}_{xy}\frac{\theta^2}{2}\begin{pmatrix} 0 & 1 \\ 1 & 0 \end{pmatrix},$$

however, no longer is identical to $\mathcal{R}_{\text{surf}}$ as this is the case for normal incidence. Therefore, Eq. (36) is not valid, because

$$\tilde{r}_{\pm}^{[s]} \simeq \tilde{r}_{\pm} \pm i\tilde{r}_{xy}\frac{\theta^2}{2} \neq \tilde{r}_{\pm} \mp i\tilde{r}_{xy}\frac{\theta^2}{2} \simeq \tilde{r}_{\pm}^{[p]},$$

where $\tilde{r}_{\pm}=\tilde{r}_{xx}\pm i\tilde{r}_{xy}=r_{\pm}\exp(i\Delta_{\pm})$. Consequently, the ϑ_i and ε_i dependence of the polar Kerr angles for almost normal incidence as evaluated from Eq. (27) by means of the circular complex polarization variable of the reflected wave

$$\tilde{\chi}_{[+,-]}^{(r)} = \frac{r_+ \exp[i(\Delta_+ - \vartheta_i)]\tan\left(\varepsilon_i + \frac{\pi}{4}\right) - i\tilde{r}_{xy}\frac{\theta^2}{2}\exp(+i\vartheta_i)}{r_- \exp[i(\Delta_- + \vartheta_i)] + i\tilde{r}_{xy}\frac{\theta^2}{2}\exp(-i\vartheta_i)\tan\left(\varepsilon_i + \frac{\pi}{4}\right)}$$
$$\times (0 < \theta \ll 1),$$

never equals $\tilde{\chi}_{[+,-]}^{(r)}$ as given by Eq. (37). This implies that for a layered system with its total magnetization oriented perpendicular to the surface, the polar Kerr rotation angle depends on the polarization state of the incident light even for the smallest possible departure of the incidence direction from the surface normal.

Except right- and left-handed circularly polarized light, for which $\varepsilon_i=\pm\pi/4$, all physically possible incident polarization states, see Eq. (20), are considered in Figs. 2 and 3. Because the azimuth of circularly polarized incident light is indeterminable, one does not need to take into account these

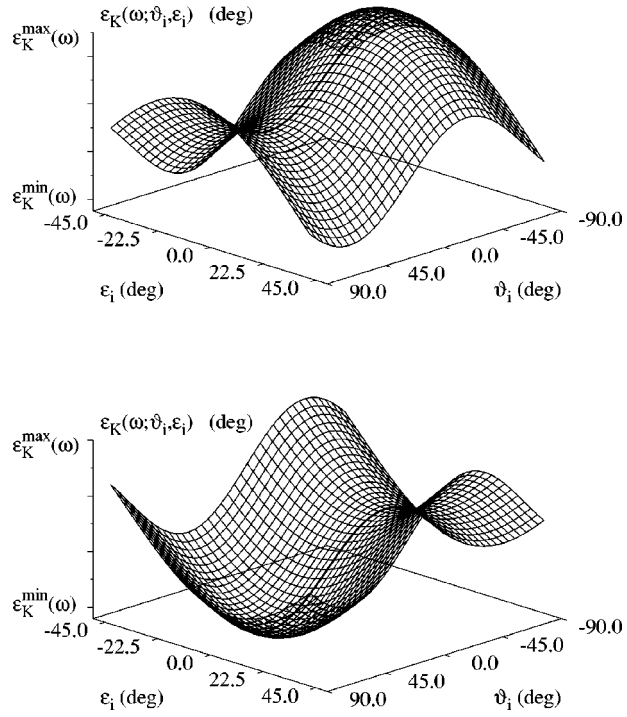

FIG. 3. As in Fig. 2 but for the Kerr ellipticity angle and arbitrary photon energies $\omega \leqslant 2.72$ eV (top) and $\omega \geqslant 2.99$ eV (bottom). Not accounted for is the left- and right-handed circularly polarized incident light, for which ϑ_i is indeterminable. Top: $\epsilon_K^{\max}=0.05°$ and $\epsilon_K^{\min}=-0.025°$, if $\omega=2.45$ eV. Bottom: $\epsilon_K^{\max}=0.025°$ and $\epsilon K\text{min}=-0.055°$, for $\omega=3$ eV.

incident polarization states. In the case of the Kerr ellipticity angle, the definition in Eq. (34) is valid for $\varepsilon_i=\pm\pi/4$, the corresponding value however, is almost vanishing. A common feature of the Kerr rotation angle $\theta_K(\omega;\vartheta_i,\varepsilon_i)$ viewed as a function of the azimuth ϑ_i and ellipticity angle ε_i is in case of the semi-infinite Ni(100) bulk ($\theta=2°$ and φ arbitrary) the independence of the photon energy ω. In contrast to the Kerr rotation angle, the shape of the Kerr ellipticity angle $\epsilon_K(\omega;\vartheta_i,\varepsilon_i)$ as function of ϑ_i and ε_i strongly depends on the photon energy ω: the curvature turns from positive to negative for photon energies between 2.72 and 2.99 eV. Below and above these values, however, the shape of $\epsilon_K(\omega;\vartheta_i,\varepsilon_i)$ is very similar to the case shown in Fig. 3. Including also $\epsilon_K(\omega;\vartheta_i,\pm\pi/4)\simeq 0$ (left- or right-handed circularly polarized incident light), independent of ω, an absolute minimum or maximum of $\epsilon_K(\omega;\vartheta_i,\varepsilon_i)$ would be seen, which however, is of secondary interest.

From the global extrema of $\theta_K(\omega;\vartheta_i,\varepsilon_i)$ and $\epsilon_K(\omega;\vartheta_i,\varepsilon_i)$ follows that Kerr spectra cannot be optimized simultaneously for all photon energies in the visible regime, since $\theta_K(\omega;\vartheta_i,\varepsilon_i)$ and $\epsilon_K(\omega;\vartheta_i,\varepsilon_i)$ have extrema at different energies. An exception from this rule seems to be an arbitrary incident linearly polarized light, see the solid bold line in Figs. 2 and 3, which for an azimuth of $\vartheta_i=+\pi/4(-\pi/4)$ maximizes (minimizes) the Kerr rotation angle and simultaneously minimizes (maximizes) the Kerr ellipticity angle for all photon energies in the visible range. In all other cases, the gain is between 5–35 % for the Kerr rotation angle and be-

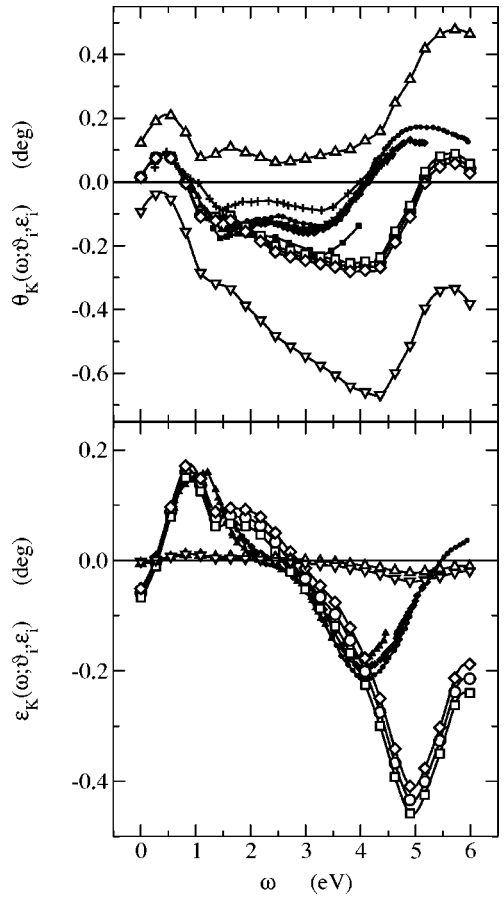

FIG. 4. Polar Kerr spectra for almost normal incidence in the case of fcc Ni(100) as obtained for arbitrary linearly polarized incident light ($\epsilon_i=0$) of azimuth $\vartheta_i=0, \pm\pi/4$ (open circles, squares and diamonds). In addition, Kerr spectra calculated for an incident light with $\vartheta_i=\pm 10°$ and $\epsilon_i=\pm 43°$ are also included (open up triangles for positive values of ϑ_i and ϵ_i and down triangles for negative values, respectively). The experimental data refer to full symbols (stars: Ref. 27, squares: Ref. 28, diamonds: Ref. 29, up triangles: Ref. 30, down triangles: Ref. 31 and pulses: Refs. 32 and 33).

tween 5–60 % for the Kerr ellipticity angle with respect to linear *p*-polarized incident light ($\vartheta_i=\varepsilon_i=0$), see also Fig. 4. No differences occur in the Kerr angles, if linear *s*- ($\vartheta_i=\pm\pi/2$) or *p*-polarized ($\vartheta_i=0$) incident light ($\varepsilon_i=0$) is used as long as the geometry is polar and the incidence is almost normal.

As can be seen in Fig. 4, changes in the Kerr rotation angle for photon energies below 2 eV and in the Kerr ellipticity angle below 1 eV that correspond to the use of arbitrary linearly polarized incident light ($\varepsilon_i=0$) of azimuth $\vartheta_i=\pm\pi/4$ are negligible with respect to those obtained with a linear *p*-polarized incident light ($\vartheta_i=\varepsilon_i=0$). For $\vartheta_i=\pi/4(\varepsilon_i=0)$ and photon energies above 2 eV, the Kerr rotation spectrum is close to the experimental one, whereas for $\vartheta_i=-\pi/4(\varepsilon_i=0)$, the Kerr rotation is largest for arbitrary linearly polarized incident light; the opposite applies for the Kerr ellipticity spectrum above 1 eV.

In comparing the theoretical Kerr spectra obtained for arbitrary linearly polarized incident light ($\varepsilon_i=0$) of azimuth $\vartheta_i=0, \pm\pi/4$ with available experimental data, one immediately observes that the calculated spectra are qualitatively similar to the experimental ones, but shifted to higher values of ω than those measured, although in the calculations the experimental lattice parameter of 6.66 a.u.[22] has been assumed for the fcc semi-infinite Ni(100) bulk. Furthermore, the theoretical Kerr ellipticity angle below 4 eV shows a better agreement with the experimental data than the Kerr rotation angle in the same range of photon energies. The obtained minimum of the Kerr ellipticity angle, however, is deeper and shifted toward higher photon energies as compared to experiments. In the literature, the discrepancies in photon energies between the theoretical and experimental Kerr spectra are rationalized by "deficiencies" in the local density approximations (LDA).[23,24] It is therefore not surprising that all other theoretical Kerr spectra of Ni obtained on the basis of band-structure methods other than the SKKR method used here,[25,26] are in pretty good agreement with the present ones: all show the same differences with respect to the experimental results, independent of whether a generalized gradient approximation (GGA), or orbital polarization (OP), or full-potential (FP) approach was applied.[22]

Because of Eq. (40), in choosing the ellipticity angle for the almost circularly polarized incident light, which in turn optimizes the Kerr rotation angle for a given photon energy, one has to take into account that the azimuth of the reflected light must be unambiguously determined even when the ellipticity of the reflected light slightly increases. For this reason, when calculating the phase of the circular complex polarization variable $\tilde{\chi}^{(r)}_{[+,-]}$ associated with the reflected light, the Kerr rotation spectrum in Fig. 4 has been optimized by considering $\varepsilon_i=\pm 43°$. This allows a change of at most $\pm 2°$ in the ellipticity angle after reflection. Correspondingly, an azimuth of $\vartheta_i=\pm 10°$ has been taken in the optimization to be as close as possible to global extrema of Kerr rotation angle below 1 eV. No doubt, that for incident polarization states characterized by $\vartheta_i=\pm 10°$ and $\varepsilon_i=\pm 43°$, one does not reach any local extremum of the Kerr rotation angle above 1 eV. However, as is shown in Fig. 4, for such chosen incident polarization states the entire Kerr rotation spectrum is significantly improved over the whole visible range, while the ellipticity remains almost unchanged. In view of Eq. (32), $\theta_K(\omega;10°,43°)>0$ means that the azimuth of the reflected light is increased by over 10° for photon energy between 1 and 6 eV, whereas $\theta_K(\omega;-10°,-43°)<0$ it is always less than 10°. Clearly enough, there are quite a lot of incident polarization states, for which the Kerr spectra can be optimized. For example, an incident light of $\varepsilon_i=15°$ and $\vartheta_i=15°$ puts the theoretical Kerr rotation spectrum closely to the experimental one, for $\varepsilon_i=\vartheta_i=30°$ the negative peak in the Kerr ellipticity spectrum around 5 eV is obtained within the experimental range.

B. Almost polar geometry and normal incidence

Another possible deviation from the ideal case of polar geometry and normal incidence occurs when the incidence is kept normal, but the magnetization of the investigated system is not exactly perpendicularly oriented to the surface.

TABLE I. Orientation of the magnetization in the atomic layers of $Co/Pt_3/Co/Pt_7/Pt(111)$. Θ_p is the rotation angle around the x axis (perpendicular to the surface normal).

atomic layer	Co	Pt	Pt	Pt	Co	Pt	Pt	Pt	Pt	Pt	Pt	Pt
Θ_p (deg.)	0	0	45	90	90	90	90	90	90	90	90	90

Such a magnetic configuration has been assumed for the fcc layered system $Co/Pt_3/Co/Pt_7/Pt(111)$, see Table I, in which Θ_p refers to the rotation angle of the orientation of magnetization in atomic layer p around the x axis (perpendicular to the surface normal).

It is well known that for normal incidence no Kerr rotation angle occurs in the longitudinal or transverse geometry. Therefore, in the present magnetic configuration of $Co/Pt_3/Co/Pt_7/Pt(111)$ only layers with an out-of-plane magnetization, but not necessarily perpendicular to the surface, contribute to the Kerr effect at normal incidence. In the chosen example, these layers are: the surface Co layer and two Pt layers immediately below. Because in the Pt layers the magnetic moment induced by Co ($M_x=0.09\ \mu_B$ and $M_z=0.40\ \mu_B$) is smaller than that of the surface Co layer ($M_x=0.00\ \mu_B$ and $M_z=2.15\ \mu_B$), the total magnetic moment of magneto-optically active layers at normal incidence shows only a small departure of about 2° from the direction perpendicular to the surface and hence the geometry can be assumed to be an almost polar one. In contrast to the previous case of polar geometry and almost normal incidence, the shape of the surfaces $\theta_K(\omega;\vartheta_i,\varepsilon_i)$ and $\epsilon_K(\omega;\vartheta_i,\varepsilon_i)$ as functions of ϑ_i and ε_i now strongly depend not only on the photon energy ω, but also on the spherical longitude φ, which in spite of $\theta=0$ places the incidence plane in reference to the global Cartesian coordinate system $S\{x,y,z\}$. However, probably due to a similar angular deviation from the ideal polar geometry and normal incidence, the Kerr rotation angle for $Co/Pt_3/Co/Pt(111)$ has global extrema for right- or left-handed almost circularly polarized incident light independent of φ, but for different azimuths ϑ_i. The Kerr ellipticity angle, on the other hand, just as in case of semi-infinite Ni(100) bulk, has global extrema for right- or left-handed almost circularly polarized incident light. An interesting aspect is that the size of these Kerr angles extrema are numerically independent of φ. For almost polar geometry and normal incidence by using arbitrary linearly polarized incident light with an azimuth $\vartheta_i=\pm\pi/4$, none of the Kerr angles reach one of the local extrema, which depending on the photon energy ω are of the order of 10–35 % for the Kerr rotation and 10–90 % in case of the Kerr ellipticity angle.

In conclusion, in case of almost polar geometry and normal incidence, there is no way — even approximately — to optimize Kerr spectra for the entire visible spectrum of photon energies as was the case for polar geometry and almost normal incidence. For this reason in Fig. 5 the relative gain in the Kerr rotation angle as function of ϑ_i with respect to the value obtained with a linear p-polarized incident light is given for different photon energies, if almost circularly polarized incident light with $\varepsilon_i=\pm 43°$ is used.

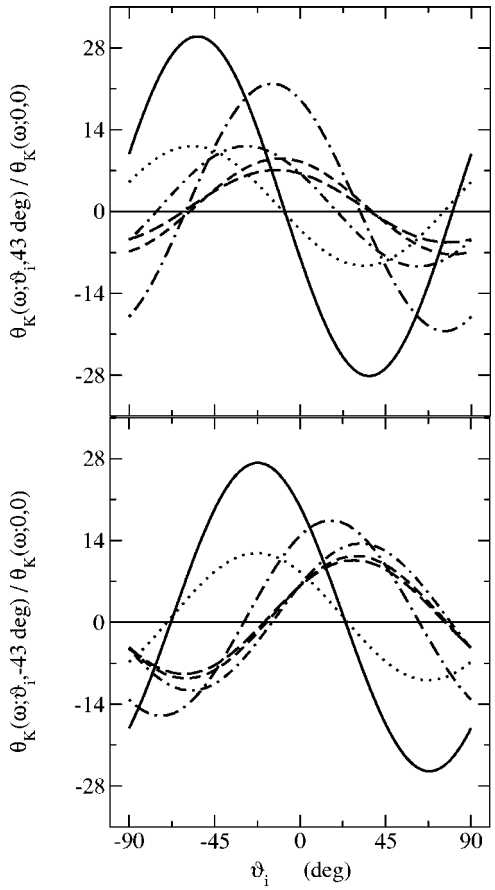

FIG. 5. Kerr rotation angles for almost polar geometry, normal incidence ($\theta=\varphi=0$) and different photon energies ω in the case of fcc $Co/Pt_3/Co/Pt(111)$ as calculated for almost circularly polarized right-(top) and left-handed (bottom) incident light ($\epsilon_i=\pm 43.0°$). The spectra are normalized to those obtained for linear p-polarized incident light ($\vartheta_i=\epsilon_i=0$). The solid, dotted, dashed, long-dashed, dot dashed, and dot long-dashed lines, correspond to photon energies of approximatively $1,2,\ldots,6$ eV, respectively.

VI. SUMMARY

Using elliptically polarized incident light for the magneto-optical Kerr effect instead of linearly polarized incident light has the advantage that with the exception of ideal polar geometry and normal incidence, in all other setups the Kerr angle can easily be increased by exploiting its dependence on the polarization state of incident light.[34] In particular for polar geometry and almost normal incidence, and almost polar geometry and normal incidence, it has to be also numerically demonstrated by using the present formalism that two global and two local extrema of the Kerr angles occur for elliptically polarized incident light whose ellipticity is considerably smaller than unity. Furthermore, it was shown that some local extrema in the Kerr angles can be reached by using an arbitrary linearly polarized incident light of proper azimuth.

ACKNOWLEDGMENTS

Financial support from the Austrian Science Ministry (Grant No. GZ 45.100), the Austrian Ministry of Economic

Affairs and Labor (Grant No. GZ 98.366/10-I/BS3/04) and in particular from the Technical University Vienna is gratefully acknowledged.

APPENDIX A: EXTREMA OF KERR ROTATION ANGLE

In order to determine the azimuth ϑ_i and ellipticity angle ε_i for which the Kerr angle, see Eq. (30) becomes extreme, the following system of two equations has to solved:

$$\frac{\partial\theta_K}{\partial\vartheta_i}=\frac{1}{2}\frac{\partial\vartheta_+}{\partial\vartheta_i}-\frac{1}{2}\frac{\partial\vartheta_-}{\partial\vartheta_i}-1=0,$$

$$\frac{\partial\theta_K}{\partial\varepsilon_i}=\frac{1}{2}\frac{\partial\vartheta_+}{\partial\varepsilon_i}-\frac{1}{2}\frac{\partial\vartheta_-}{\partial\varepsilon_i}-1=0,$$

where according to Eq. (31)

$$\frac{\partial\vartheta_\pm}{\partial\zeta}=\frac{1}{Z_\pm^2}\left(X_\pm\frac{\partial Y_\pm}{\partial\zeta}-Y_\pm\frac{\partial X_\pm}{\partial\zeta}\right)\ (\zeta=\vartheta_i,\varepsilon_i). \tag{A1}$$

In Eq. (A1) the derivatives of $X_\pm$ and $Y_\pm$ are given by

$$\frac{\partial X_\pm}{\partial\vartheta_i}=(I_\pm^{[p]}\tan\varepsilon_i\pm I_\pm^{[s]})(1+\tan^2\vartheta_i),$$

$$\frac{\partial X_\pm}{\partial\varepsilon_i}=(\pm R_\pm^{[s]}+I_\pm^{[p]}\tan\vartheta_i)(1+\tan^2\varepsilon_i),$$

$$\frac{\partial Y_\pm}{\partial\varepsilon_i}=(R_\pm^{[p]}\tan\varepsilon_i\pm R_\pm^{[s]})(1+\tan^2\vartheta_i),$$

$$\frac{\partial Y_\pm}{\partial\varepsilon_i}=(R_\pm^{[p]}\tan\vartheta_i\mp I_\pm^{[s]})(1+\tan^2\varepsilon_i) \tag{A2}$$

while $Z_\pm$ follows from Eq. (28),

$$\begin{aligned}Z_\pm^2=&(r_\pm^{[p]})^2(1+\tan^2\vartheta_i\tan^2\varepsilon_i)+(r_\pm^{[s]})^2(\tan^2\vartheta_i+\tan^2\varepsilon_i)\\&\pm2(R_\pm^{[p]}R_\pm^{[s]}+I_\pm^{[p]}I_\pm^{[s]})(1+\tan^2\vartheta_i)\tan\varepsilon_i\\&\pm2(R_\pm^{[p]}I_\pm^{[s]}-R_\pm^{[s]}I_\pm^{[p]})\tan\vartheta_i(1-\tan^2\varepsilon_i).\end{aligned} \tag{A3}$$

In using the expressions given in Eqs. (A2) and (A3) explicitly in Eq. (A1), one obtains

$$\begin{aligned}\frac{\partial\vartheta_\pm}{\partial\vartheta_i}=&\frac{1+\tan^2\vartheta_i}{Z_\pm^2}\{[(r_\pm^{[p]})^2+(r_\pm^{[s]})^2]\tan\varepsilon_i\\&\pm[R_\pm^{[p]}R_\pm^{[s]}+I_\pm^{[p]}I_\pm^{[s]}](1+\tan^2\varepsilon_i)\},\end{aligned}$$

$$\begin{aligned}\frac{\partial\vartheta_\pm}{\partial\varepsilon_i}=&\frac{1+\tan^2\varepsilon_i}{Z_\pm^2}\{[(r_\pm^{[p]})^2-(r_\pm^{[s]})^2]\tan\vartheta_i\\&\mp[R_\pm^{[p]}I_\pm^{[s]}-R_\pm^{[s]}I_\pm^{[p]}](1-\tan^2\vartheta_i)\}\end{aligned}$$

such that

$$\begin{aligned}\sum_{j=\pm}j\frac{1+\tan^2\vartheta_i}{Z_j^2}\{&[(r_j^{[p]})^2+(r_j^{[s]})^2]\tan\varepsilon_i\\&+j[R_j^{[p]}R_j^{[s]}+I_j^{[p]}I_j^{[s]}](1+\tan^2\varepsilon_i)\}=2,\end{aligned}$$

$$\begin{aligned}\sum_{j=\pm}j\frac{1+\tan^2\varepsilon_i}{Z_j^2}\{&[(r_j^{[p]})^2-(r_j^{[s]})^2]\tan\vartheta_i\\&-j[R_j^{[p]}I_j^{[s]}-R_j^{[s]}I_j^{[p]}](1-\tan^2\vartheta_i)\}=2.\end{aligned}$$

Consider now arbitrary linearly polarized incident light ($\varepsilon_i=0$), for which

$$\begin{aligned}Z_j^2|_{\varepsilon_i=0}=&(r_j^{[s]})^2\tan^2\vartheta_i+2j(R_j^{[p]}I_j^{[s]}-R_j^{[s]}I_j^{[p]})\tan\vartheta_i\\&+(r_j^{[p]})^2\ (j=\pm).\end{aligned}$$

The only equation left to be solved with respect to ϑ_i reduces therefore to

$$\sum_{j=\pm}\frac{1+\tan^2\vartheta_i}{Z_j^2}(R_j^{[p]}R_j^{[s]}+I_j^{[p]}I_j^{[s]})=2,$$

from which immediately follows that the Kerr angle for an *s* or *p* wave is extreme only for particular combinations of incidence and optical properties of the system investigated, namely,

$$\left.\frac{\partial\theta_K(\varepsilon_i=0)}{\partial\vartheta_i}\right|_{\vartheta_i=\pm\pi/2}=0\ \text{if and only if}\ \sum_{j=\pm}\frac{R_j^{[p]}R_j^{[s]}+I_j^{[p]}I_j^{[s]}}{(R_j^{[s]})^2+(I_j^{[s]})^2}=2$$

and

$$\left.\frac{\partial\theta_K(\varepsilon_i=0)}{\partial\vartheta_i}\right|_{\vartheta_i=0}=0\ \text{if and only if}\ \sum_{j=\pm}\frac{R_j^{[p]}R_j^{[s]}+I_j^{[p]}I_j^{[s]}}{(R_j^{[p]})^2+(I_j^{[p]})^2}=2.$$

[1] J. Kerr, Rep. Brit. Assoc. Adv. Sci. 40 (1876); Philos. Mag. **3**, 321 (1877); **5**, 161 (1878).

[2] M. Mansuripur, *The Principles of Magneto-Optical Recording* (Cambridge University Press, Cambridge, 1995).

[3] W. Reim and J. Schoenes, in *Magneto-optical Spectroscopy of f-electron Systems, Ferromagnetic Materials*, edited by K. H. J. Buschow and E. P. Wohlfarth (North-Holland, Amsterdam, 1990), Vol. 5, Chap. 2, p. 133.

[4] A. K. Zvezdin and V. A. Kotov, *Modern Magnetooptics and Magnetooptical Materials, Studies in Condensed Matter Physics* (Institute of Physics Publishing, Bristol, 1997).

[5] P. M. Oppeneer, Habilitationsschrift, Technische Universität Dresden, 1999.

[6] A. Vernes, L. Szunyogh, and P. Weinberger, Phase Transitions **75**, 167 (2002).

[7] J. D. Jackson, *Classical Electrodynamics* (Wiley, New York, 1975).

[8] L. D. Landau and E. M. Lifshitz, *Electrodynamics of Continuous Media*, Vol. 8 of *Course of Theoretical Physics* (Butterworth-Heinemann, Oxford, 1999).

[9] M. Mansuripur, J. Appl. Phys. **67**, 6466 (1990).
[10] A. Vernes, L. Szunyogh, and P. Weinberger, Phys. Rev. B **66**, 214404 (2002).
[11] R. M. A. Azzam and N. M. Bashara, *Ellipsometry and Polarized Light* (North-Holland, Amsterdam, 1999).
[12] G. Metzger, P. Pluvinage, and R. Torguet, Ann. Phys. (Paris) **10**, 5 (1965).
[13] J. Zak, E. R. Moog, C. Liu, and S. D. Bader, Phys. Rev. B **43**, 6423 (1991).
[14] C.-Y. You and S.-C. Shin, J. Appl. Phys. **84**, 541 (1998).
[15] R. Urban, M. Nyvlt, S. Visnovsky, J. Ferre, D. Renard, and M. Galtier, J. Magn. Magn. Mater. **198-199**, 506 (1999).
[16] *Handbook of Mathematical Functions with Formulas, Graphs and Mathematical Tables*, edited by M. Abramowitz and I. A. Stegun (Dover, New York, 1972).
[17] A. Vernes, L. Szunyogh, and P. Weinberger, Phys. Rev. B **65**, 144448 (2002).
[18] A. Vernes, L. Szunyogh, and P. Weinberger, J. Magn. Magn. Mater. **240**, 216 (2002).
[19] A. Vernes, L. Szunyogh, and P. Weinberger, J. Phys.: Condens. Matter **13**, 1529 (2001).
[20] L. Szunyogh and P. Weinberger, J. Phys.: Condens. Matter **11**, 10 451 (1999).
[21] L. Szunyogh, B. Újfalussy, P. Weinberger, and J. Kollár, Phys. Rev. B **49**, 2721 (1994); L. Szunyogh, B. Újfalussy, and P. Weinberger, *ibid.* **51**, 9552 (1995); B. Újfalussy, L. Szunyogh, and P. Weinberger, *ibid.* **51**, 12 836 (1995).
[22] J. Kunes and P. Novak, J. Phys.: Condens. Matter **11**, 6301 (1999).
[23] N. Mainkar, D. A. Browne, and J. Callaway, Phys. Rev. B **53**, 3692 (1996).
[24] P. M. Oppeneer, T. Maurer, J. Sticht, and J. Kübler, Phys. Rev. B **45**, 10 924 (1992).
[25] P. M. Oppeneer and V. N. Antonov, in *Spin-orbit Influenced Spectroscopies of Magnetic Solids*, Vol. 466 of *Lecture Notes in Physics*, edited by H. Ebert and G. Schütz (Springer, Berlin, 1996), p. 29.
[26] A. Delin, O. Eriksson, B. Johansson, S. Auluck, and J. M. Wills, Phys. Rev. B **60**, 14 105 (1999).
[27] K. Nakajima, H. Sawada, T. Katayama, and T. Miyazaki, Phys. Rev. B **54**, 15 950 (1996).
[28] G. Q. Di and S. Uchiyama, J. Appl. Phys. **75**, 4270 (1994).
[29] S. Visnovsky, V. Parzek, M. Nyvlt, P. Kielar, V. Prosser, and R. Krishnan, J. Magn. Magn. Mater. **127**, 135 (1993).
[30] P. G. van Engen, Ph.D. thesis, Technical University Delft, Delft, 1983.
[31] P. G. van Engen, K. H. J. Buschow, and M. Erman, J. Magn. Magn. Mater. **30**, 374 (1983).
[32] G. S. Krinchik and V. A. Artemjev, Sov. Phys. JETP **26**, 1080 (1968).
[33] G. S. Krinchik and V. A. Artemjev, J. Appl. Phys. **39**, 1276 (1968).
[34] The theoretical concept of increasing Kerr angles was filed as a patent (Österreichisches Patentamt, AZ. 1393/2004).